The contact force of 43 N was applied between the contacts, while the gap length at the opening period was set to 300 μm. After turning off MOSFET1, MOSFET2 was turned on; then, the charge stored in the actuator was discharged at the time constant determined by the discharge resistor. The gap length between the contacts was measured by a laser displacement sensor (KEYENCE, LK-H055, LK-G600V). The gap length oscillated as shown in Fig. 4. The maximum gap length of 0.42 mm was obtained at 1.2 ms.

Fig. 5 shows the experimental circuit for the hybrid switch. The maximum voltage and current of the power source were 20 V and 800 A, respectively.

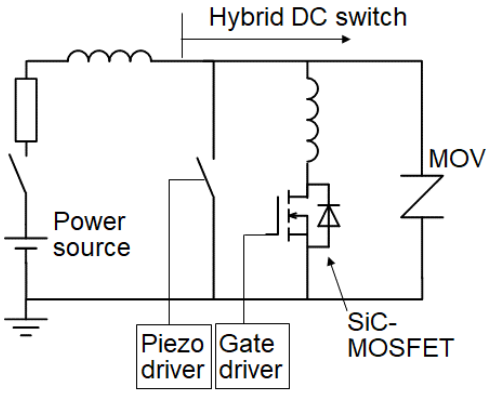

Fig. 5 Experimental setup for the hybrid DC switch.

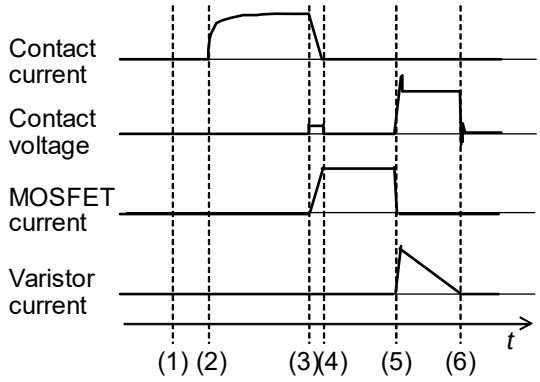

Fig. 6 Interrupting sequence.

The opening sequence of the hybrid switch is shown in Fig. 6. The contacts are initially closed at time (1). Then, the power source turns on to apply a DC voltage to the circuit at time (2). The contact current increases with a time constant of determined by the circuit inductance and resistance. When the piezoelectric actuator is discharged at time (3), the contact starts to open, the contact current decreases, and the MOSFET current increases in turn. The contact voltage exhibits the voltage of a molten bridge; this value is the same as the turn-on voltage of the SiC-MOSFET. After the commutation period, a sufficient gap length is needed to prevent the arc generation between the contacts. Finally, the SiC-MOSFET turns off at time (5), and then, the MOSFET current is commutated to the varistor, which dissipates the inductive energy in the circuit. The interrupting time of the hybrid switch corresponds to the time from (3) to (6), and its duration could be reduced to less than a few milliseconds.

4. Results and Discussion

A. Suppression of Making Arc

To suppress the generation of an arc discharge, the SiC-MOSFET is turned on before closing the contacts. Fig. 7 shows the contact voltages with and without turning on the SiC-MOSFET at a current flow of 400 A. Without turning off the SiC-MOSFET, the contact voltage at time zero is equal to the circuit voltage of 20 V. As the gap length decreased, an arc discharge was generated at 3.4 ms, and the contact voltage fluctuated and dropped to approximately 16 V; this value shows the arc voltage. At time 5.1 ms, the contacts seemed to become attached to each other, and the contact voltage gradually decreased to 0 V.

In the case that the SiC-MOSFET was turned-on before closing, the contact voltage or the turn-on voltage of SiC-MOSFET was 3.5 V at a current flow of 400 A. The contact voltage decreased to 2.0 V at time 3.4 ms, because a part of the current flowed in the contacts. During the closing process, no arc discharge was generated.

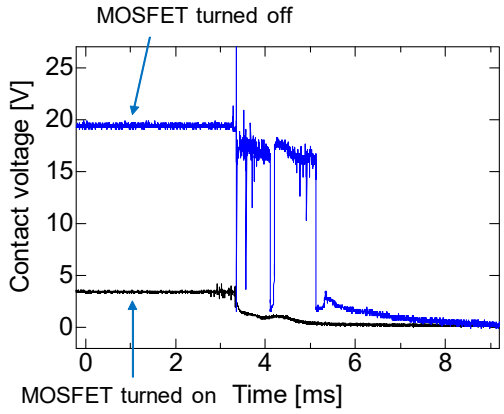

Fig. 7 Contact voltages with and without turning on the SiC-MOSFET during closing process of the hybrid switch.

B. Suppression of Breaking Arc and Arc-free Interruption

The detailed changes in contact voltage and current waveforms during the commutation period are shown in Fig. 8. The initial contact current was 400 A. After turning on the SiC-MOSFET, a portion of the contact current flowed into the SiC-MOSFET; therefore, the contact current decreased. When the piezo actuator started to separate the contacts, the contact force began to decrease; therefore, the contact voltage gradually increased. When the maximum temperature of the contact surface reached the melting point, the contact voltage showed the stepwise increase at time 2.3 ms. Because of the decrease of the rate of increase of the contact voltage decreased in the following period, and the contact voltage reached approximately 1.9 V, is below the boiling

voltage of tungsten (2.1 V). During the commutation period, arc discharges were not observed.

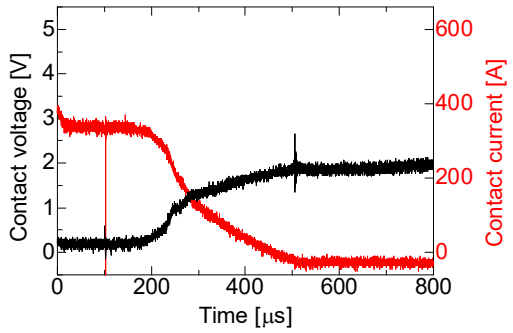

Fig. 8 Contact voltage and current waveforms during commutation of 400 A.

Fig. 9 shows the contact voltage and current waveforms during the commutation of the 500 A current. The stepwise increase and decrease of contact voltage and current were observed after 2.1 ms. At the end of the commutation, a voltage spike was observed at 4.5 ms. The peak voltage exceeded 5 V; thus, the transient breakdown or an arc discharge was generated at this time. The duration of the discharge was short, and the contact voltage reached 2.5 V, exceeding the boiling voltage of tungsten. From these experiments, the maximum arc-free commutation current is 400 A for the current parameters of the hybrid switch.

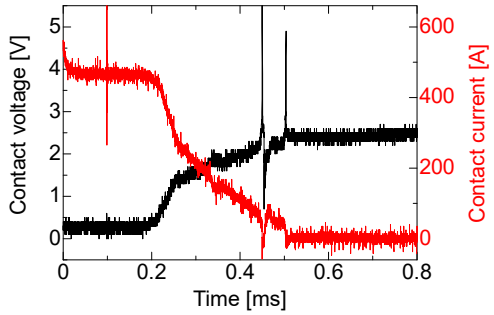

Fig. 9 Current commutation of 500 A DC with short duration arc.

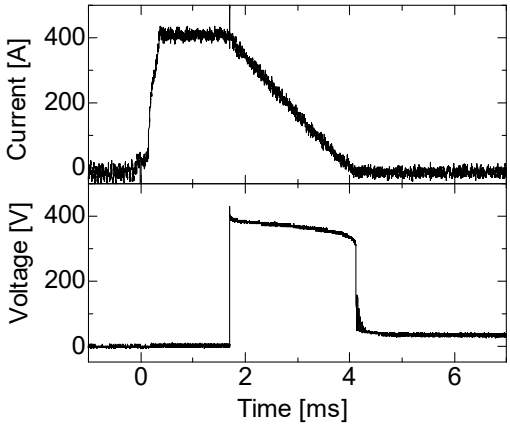

Fig. 10 Contact current and voltage waveforms at arc-free current interruption of 400 A.

The arc-free current interruption of 400 A was demonstrated as shown in Fig. 10 [11]. The switch current, which is the same as the contact current at this period, started to flow at time 0 ms, then reached 400 A at time 0.4 ms. The commutation period is within 0.3 ms, and contact voltage is below 3 V, as shown in Fig. 8; thus, detailed change in the contact voltage is not observed in Fig. 10. At time 1.7 ms, the SiC-MOSFET was turned off, and the switch voltage increased to 400 V, which is the limiting voltage of the varistors. The inductive energy of the circuit was dissipated in the varistor, and the switch current gradually decreased to zero. The interrupting time of 400 A was 2.4 ms, without generating arc discharges.

5. Conclusion

Arc-free on/off switching of 400 A direct current was demonstrated using a hybrid DC switch which consists of tungsten-clad copper contacts with a SiC-MOSFET module and varistors. The tungsten part of the contacts increases the boiling voltage of the contacts, and the copper part decreases the maximum temperature at the contact spot. Both the making and breaking arc discharges were suppressed by this hybrid switch. The commutation period during the opening process of the switch was below 0.3 ms, and the current interrupting period was 2.4 ms for 400 A.

Acknowledgement

This work was supported by JSPS KAKENHI Grant Number JP18H01420.

References

[1] V. A. Prabhala, B. P. Baddipadiga, P. Fajri, and M. Ferdowsi, “An Overview of Direct Current Distribution System Architectures & Benefits,” Energies, Vol. 11, 2463, 2018.
[2] J.C. Ferreira, V. Monteiro, J.L. Afonso, and A. Silva, “Smart Electric Vehicle Charging System,” IEEE Intelli. Vehicles Sympo. (IV), pp. 758–763, 2011.
[3] E. Skjong, E. Rodskar, M. Molinas, T.A. Johansen, J. Cunningham, “The Marine Vessel’s Electrical Power System: From its Birth to Present Day,” Proc. IEEE, Vol. 103, No. 12, pp. 2410–2424, 2015.
[4] P. J. Theisen, S. Krstic, “270-V DC Hybrid Switch,” IEEE Trans. CHMT, Vol. 9, No. 1, pp. 97–100, 1986.
[5] S. Greitzke, and M. Lindmayer, Commutation and Erosion in Hybrid Contactors Systems,” IEEE Trans. CHMT, Vol. 8, No. 1, pp. 34–39, 1985.
[6] R. Nakayama, C. Ou, S. Zen, and K. Yasuoka, “Dielectric strength of electric contacts after short-duration arc in a hybrid DC circuit breaker,” IWHV 2018, ED-18-095, 2018.
[7] T. Morita, “ArcFree Technology - Toward a DC Civilization. Internet,” https://www.sonycsl.co.jp/tokyo/3088/, 2015.
[8] R. Holm, “Electric Contacts,” Fourth edition, Springer Verlag, 1967.
[9] K. Yasuoka, Y. Tsuboi, T. Hayakawa, and N. Takeuchi, “Arcless Commutation of a Hybrid DC Breaker by Contact voltage of Molten Metal Bridge,” IEEE Trans. CPMT, Vol. , No. 99, pp. 1–6, 2017.
[10] P.G. Slade, “Electrical Contacts: Principles and Applications,” Second Edition, CRC Press, p. 586, 2017.
[11] Y. Yamada, M. Chen, and K. Yasuoka, “Development of Copper-Tungsten Clad-contacts for 400 A arc-less Switching of Hybrid DC Switch”, IEEJ Trans. PE, Vol. 139, No. 9, pp. 592–597, 2019. (in Japanese)